Turk J Phys
25 (2001) , 293 – 307.
© TÜBİTAK

# Photospheric Line Profiles in Deneb (A2 Iae)

**Berahitdin ALBAYRAK, Cemal AYDIN**
*Ankara University, Faculty of Science,*
*Department of Astronomy and Space Sciences, 06100, Tandoğan, Ankara, TURKEY*
**Dursun KOÇER**
*İstanbul University, Faculty of Science,*
*Department of Astronomy and Space Sciences, 34452, University, İstanbul, TURKEY*

Received 16.06.2000

**Abstract**

In this study, the strong lines were examined to determine the effect of velocity gradient due to mass loss on the line profiles in the atmosphere of Deneb. The lines are formed in the optical depth range -1.14 < log $\tau$ < -0.14. None were found to exibit any asymmetry.

**Key Words:** stars: individual: Deneb - stars: line profiles.

## 1. Introduction

Deneb, one of the most important stars in our Galaxy, is the prototype of the early A-type supergiants, which are among the most luminous stars in the Milky Way and in other spiral galaxies. It is readily accessable to Northern hemisphere observers. It is also relatively sharp-lined and unreddened. Many important astrophysical studies have involved Deneb. Deneb is known by a variety of names including $\alpha$ Cygni, 50 Cygni, HR 7924, HD 197345, BD $+44^o$ 3541, GC 28846, SAO 49941, ADS 14172, FK4 777, GCRV 12971, and HIP 102098. Its apparent visual magnitude is 1.2966 (ESA [1]), its 2000.0 equatorial coordinates are $\alpha = 20^h\ 41^m\ 25^s.821$, and $\delta = 45^o\ 16^{'}\ 49^{''}.13$ and its galactic coordinates are $l = 84^o.28$ and $b = +2^o.0$. Its spectral type is given as A2 Ia by almost all modern classifiers (see Albayrak [2]). It is appropriate to add an e to the spectral type as emission line cores are seen in at least $H_\alpha$. Buscombe [3], Chadeau [4], Groth [5], Taffara [6], Zverko [7], Samedov [8], Takeda et al. [9] and more recently Albayrak [10] have studied the photospheric chemical composition of Deneb. Albayrak [10] found only a small enrichment in the metal abundances for Deneb relative to Sun.

## 2. The Spectra

Reticon and CCD DAO spectrograms, with a resolution of 0.072 Å were used: they covered 67 and 63 Å, respectively, in the region $\lambda\lambda 3830 - 5212$. Using the exposures of an incandescent lamp, the exposures were flat fielded. A central stop removed light from the beam as does the secondary mirror of the telescope. The spectra were rectified using the interactive computer graphics program REDUCE (Hill & Fisher [11]). In a few regions, we used single spectra with signal-to-noise ratios of about 750. These values were found by measuring line free continuum regions. Often the spectra for a given region are co-added (Hill & Adelman [12]) to increase the signal-to-noise ratio to 900 or more. The lines found, their wavelengths, line widths, line depths, and probable identifications will be present as a spectral atlas (Albayrak et al. [13]). This should be a useful guide for other A-type supergiants.

## 3. Line Asymmetries

The atmospheres of all highly luminous stars are unstable and show large rates of mass loss. Deneb is a typical representative of such stars and its mass loss rate has been determined several times (see Albayrak [2]). The wide range of values reflect the use of different methods and the lack of understanding of the detailed structure of the stellar wind. The mass loss mechanism and the origin of the wind are not yet known in A supergiants. Radiation pressure almost certainly plays role in accelerating the flow (Achmad et al. [14]), but nonradial pulsations and other mass motions within the photosphere and outer envelop are likely to be important in initiating the wind (Lucy [15], Wolff [16]).

Lamers & Achmad [17] investigated the effect of stellar mass loss on the photospheric lines of supergiants of spectral types O to late F (including Deneb) and explained that a high mass loss rate produces a velocity gradient in the photospheres of supergiants which affects the line shapes. Strong lines ($W_\lambda > 200$ mÅ) formed in a high layer are sensitive to the velocity gradient due to mass loss in the atmosphere and therefore these lines become asymmetric (Achmad et al. [14]).

Thus, spectral line asymmetries are an extremely powerful tool for investigating photospheric velocity fields. To determine the asymmetry of a spectral line, one can reverse the profile on itself. The strong lines (those greater than 240 mÅ) were examined for asymmetries. Those that are significantly blended with lines of other elements were not considered. Table 1 lists these selected strong lines, their equivalent widths and the mean depths of formation in the atmosphere. Program WIDTH9 (Kurucz, private communications) was used to calculate the mean depth of formation for each one line. We reversed every line profile on itself using the interactive software language IDL. Figures (1 to 22) show that the strong unblended lines do not exhibit any asymmetry which are formed within the range of $\log \tau$ = -1.41 and -0.14 in Deneb. Thus, these lines do not become asymmetric due to the velocity gradient in the atmosphere of Deneb.

**Table 1**. The strong lines in Deneb selected from the studied.

| line ($\lambda$) | $W_\lambda$ ($m\AA$) | log $\tau$ |
|---|---|---|
| Si II 3862.595 | 332.6 | - 0.44 |
| Ti II 3913.477 | 284.8 | - 0.82 |
| Ca II 3933.664 | 1256.3 | - 1.41 |
| Si II 4128.067 | 243.1 | - 0.14 |
| Si II 4130.893 | 251.3 | - 0.15 |
| Fe II 4178.855 | 277.8 | - 0.33 |
| Ti II 4300.064 | 265.9 | - 0.68 |
| Fe II 4303.166 | 314.1 | - 0.43 |
| Fe II 4385.381 | 279.1 | - 0.33 |
| Ti II 4395.004 | 257.3 | - 0.66 |
| Mg II 4481.129,.327 | 658.5 | - 1.09 |
| Fe II 4508.283 | 333.8 | - 0.49 |
| Fe II 4515.337 | 300.4 | - 0.39 |
| Fe II 4520.225 | 292.1 | - 0.38 |
| Fe II 4522.634 | 393.9 | - 0.66 |
| Fe II 4555.890 | 352.1 | - 0.54 |
| Cr II 4558.660 | 312.8 | - 0.36 |
| Ti II 4571.957 | 241.5 | - 0.57 |
| Cr II 4588.220 | 272.7 | - 0.27 |
| Fe II 4923.930 | 566.3 | - 1.17 |
| Fe II 5018.450 | 516.2 | - 1.02 |
| Fe II 5197.559 | 287.1 | - 0.39 |

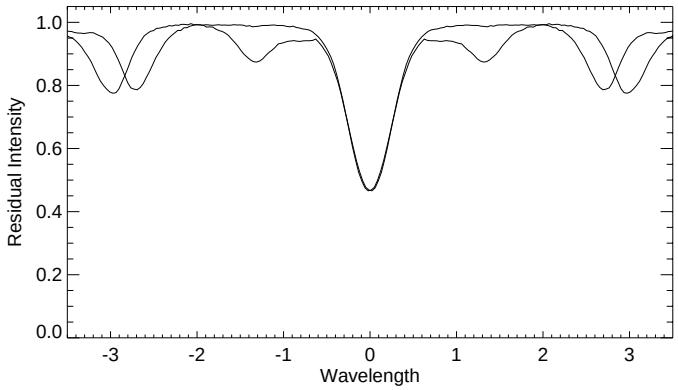


**Figure 1.** The reversed profile of Si II $\lambda$3862 in Deneb to detect the asymmetry that results in a symmetric spectral line.

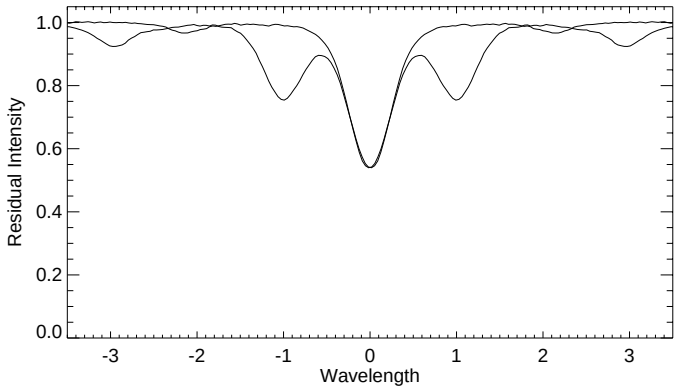


**Figure 2.** The reversed profile of Ti II $\lambda$3913 in Deneb. Otherwise, the same as in Fig. 1.

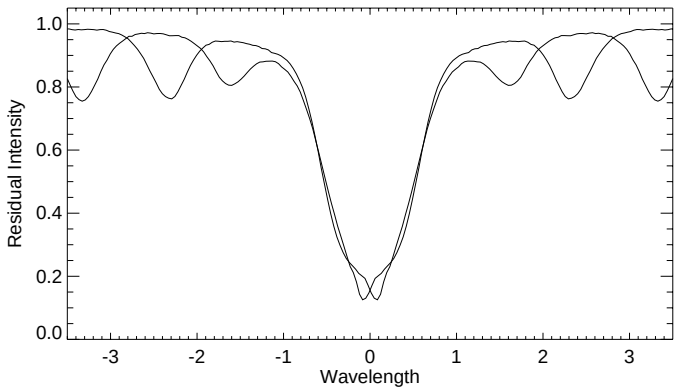


**Figure 3.** The reversed profile of Ca II $\lambda$3933 in Deneb. Otherwise, the same as in Fig. 1. Note near the core, an interstellar component is seen.

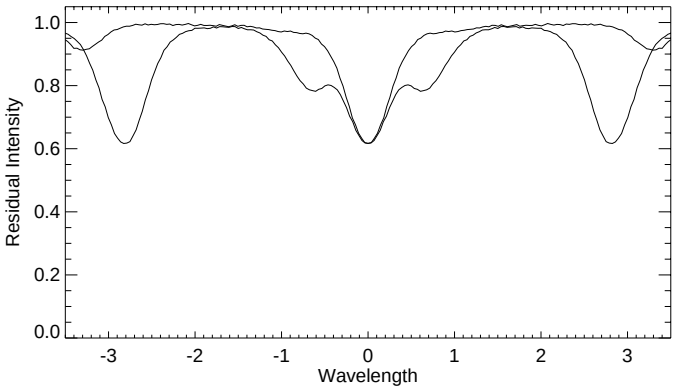


**Figure 4.** The reversed profile of Si II $\lambda$4128 in Deneb. Otherwise, the same as in Fig. 1.

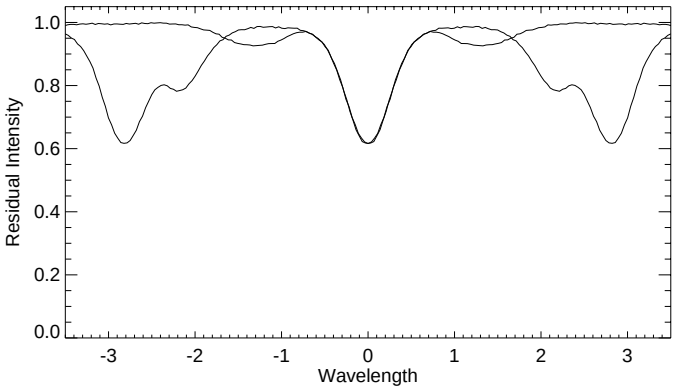


**Figure 5.** The reversed profile of Si II $\lambda$4130 in Deneb. Otherwise, the same as in Fig. 1.

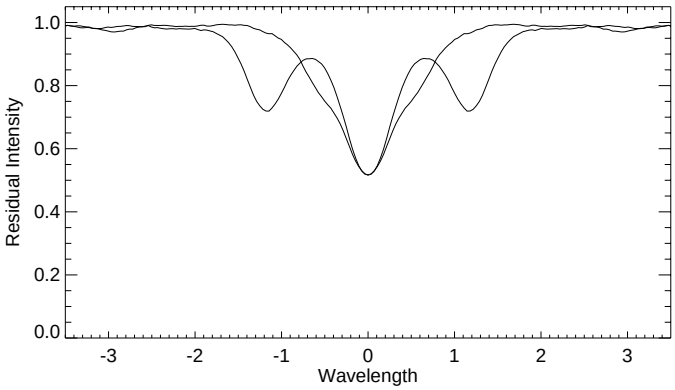


**Figure 6.** The reversed profile of Fe II $\lambda$4178 in Deneb. Otherwise, the same as in Fig. 1.

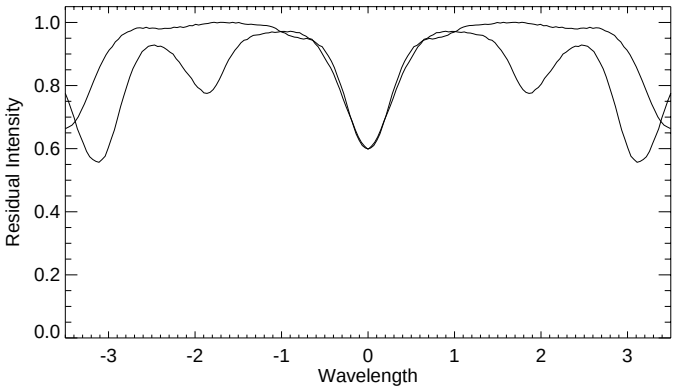


**Figure 7.** The reversed profile of Ti II $\lambda$4300 in Deneb. Otherwise, the same as in Fig. 1.

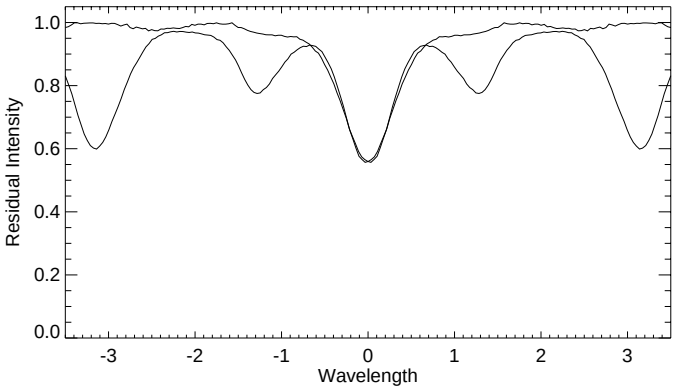


**Figure 8.** The reversed profile of Fe II $\lambda$4303 in Deneb. Otherwise, the same as in Fig. 1.

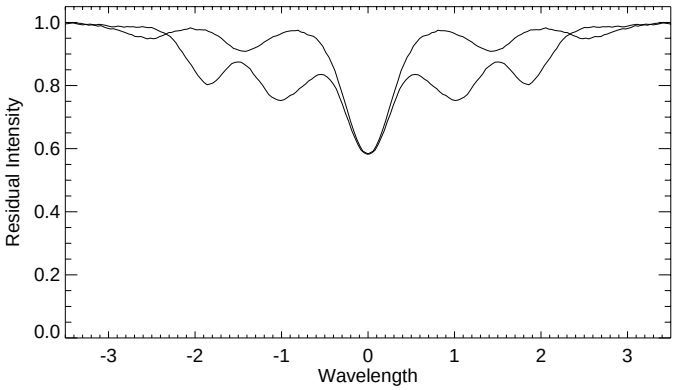


**Figure 9.** The reversed profile of Fe II $\lambda$4385 in Deneb. Otherwise, the same as in Fig. 1.

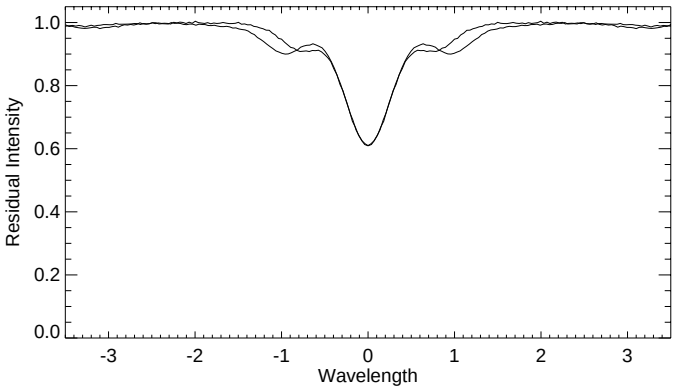


**Figure 10.** The reversed profile of Ti II $\lambda$4395 in Deneb. Otherwise, the same as in Fig. 1.

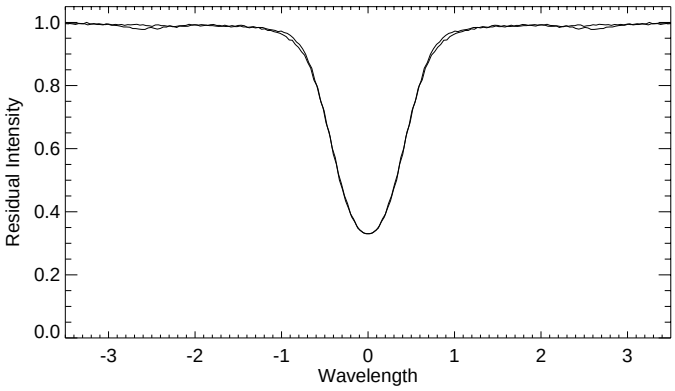


**Figure 11.** The reversed profile of Mg II $\lambda$4481 in Deneb. Otherwise, the same as in Fig. 1.

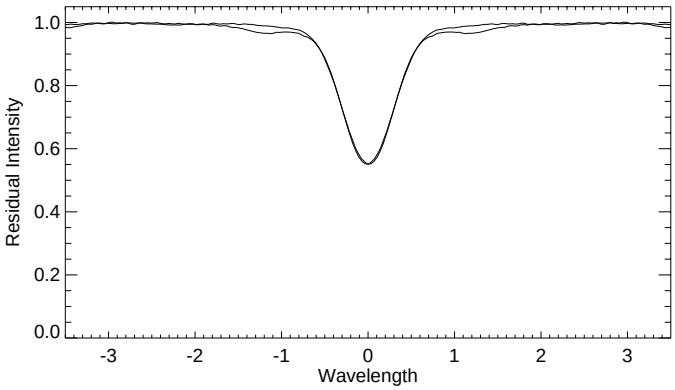


**Figure 12.** The reversed profile of Fe II $\lambda$4508 in Deneb. Otherwise, the same as in Fig. 1.

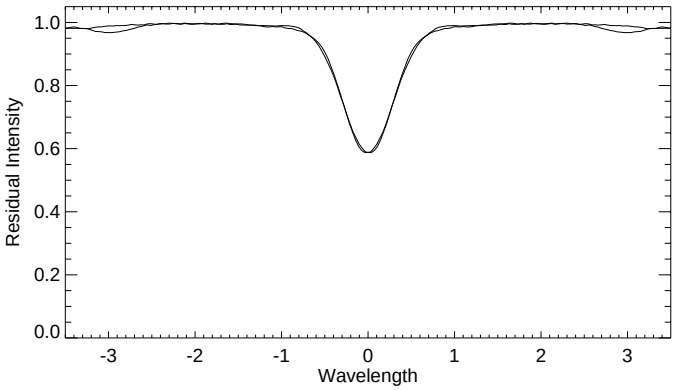


**Figure 13.** The reversed profile of Fe II $\lambda$4515 in Deneb. Otherwise, the same as in Fig. 1.

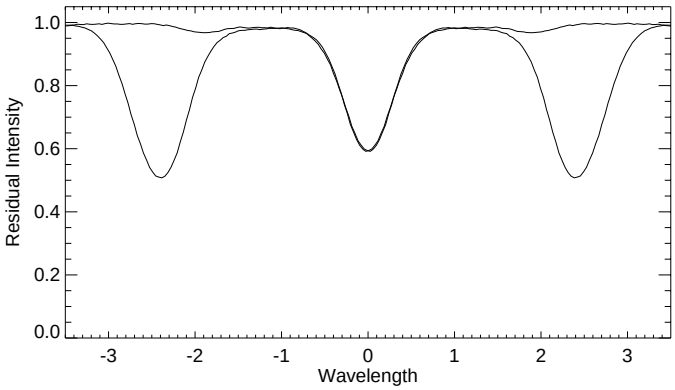


**Figure 14.** The reversed profile of Fe II $\lambda$4520 in Deneb. Otherwise, the same as in Fig. 1.

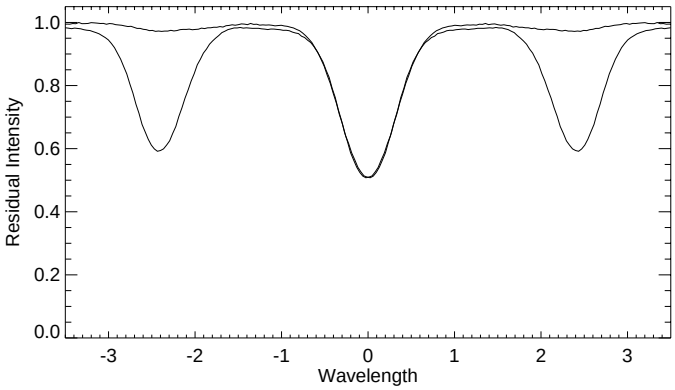


**Figure 15.** The reversed profile of Fe II $\lambda$4522 in Deneb. Otherwise, the same as in Fig. 1.

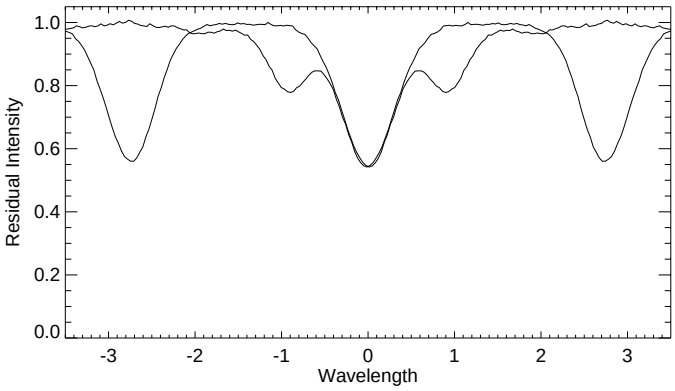


**Figure 16.** The reversed profile of Fe II $\lambda$4555 in Deneb. Otherwise, the same as in Fig. 1.

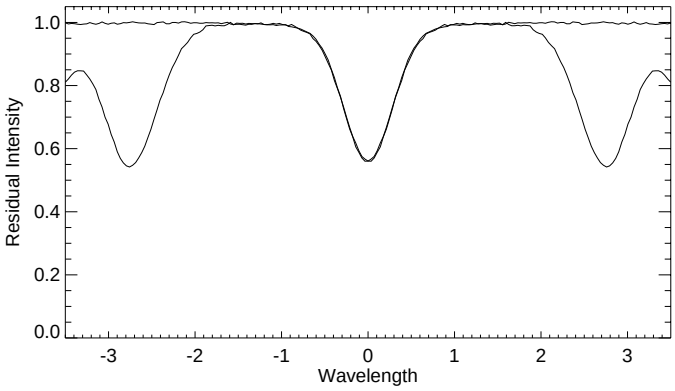


**Figure 17.** The reversed profile of Cr II $\lambda$4558 in Deneb. Otherwise, the same as in Fig. 1.

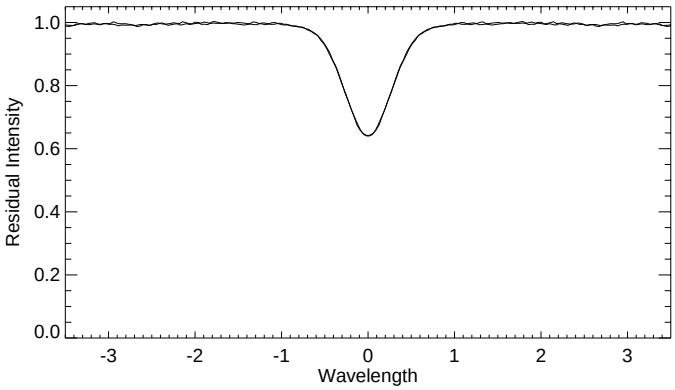


**Figure 18.** The reversed profile of Ti II $\lambda$4571 in Deneb. Otherwise, the same as in Fig. 1.

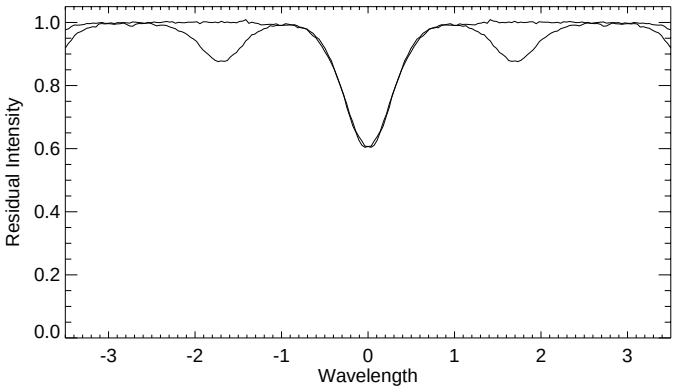


**Figure 19.** The reversed profile of Cr II $\lambda$4588 in Deneb. Otherwise, the same as in Fig. 1.

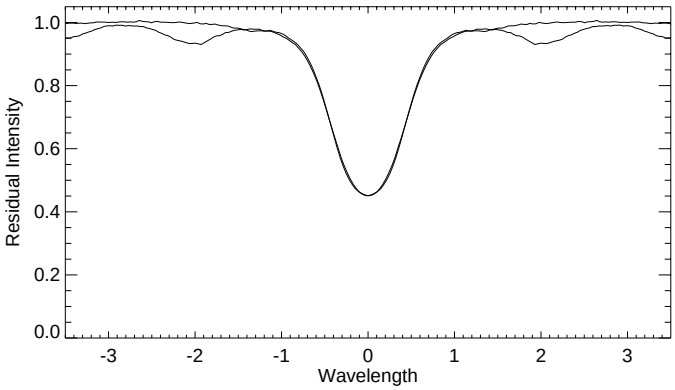


**Figure 20.** The reversed profile of Fe II $\lambda$4923 in Deneb. Otherwise, the same as in Fig. 1.

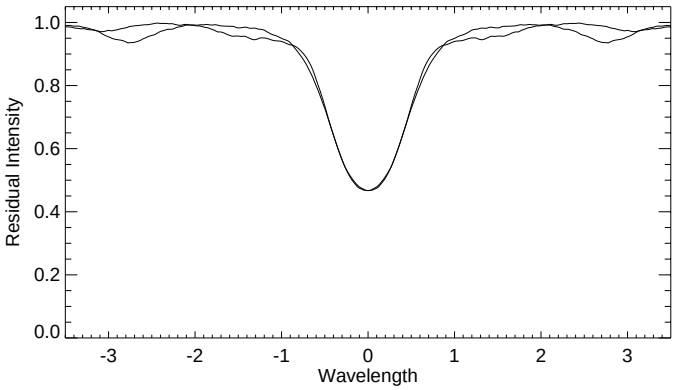


**Figure 21.** The reversed profile of Fe II $\lambda$5018 in Deneb. Otherwise, the same as in Fig. 1.

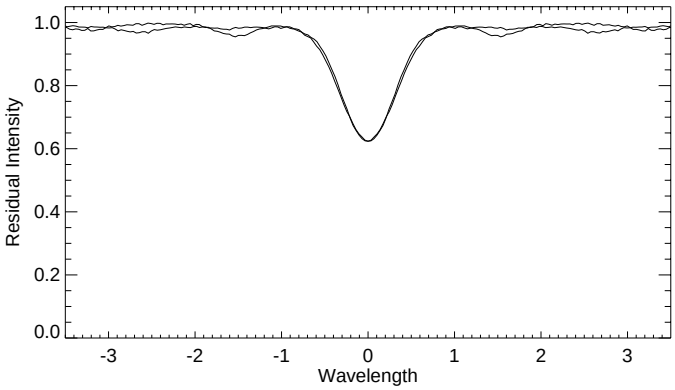


**Figure 22.** The reversed profile of Fe II $\lambda$5197 in Deneb. Otherwise, the same as in Fig. 1.

## 4. Conclusions

We examined the strong lines (equivalent widths greater than 240 mÅ) to investigate the effect of stellar mass loss on the photospheric lines of Deneb. Each line profile was reversed on itself to detect the asymmetry, but nothing significant one was found. But, this does not guarentee that any strong line, formed further out ($\log \tau <$ -1.41) from the surface, will also be symmetric (see Lamers & Achmad [17], and Achmad et al. [14]).

## Acknowledgements

Special thanks to Dr. Saul J. Adelman for his generous help in this study. *TÜBİTAK, The Scientific and Thechnical Research Council of Turkey*, is also gratefully acknowledged for the support given to this work.

## References

[1] ESA, *The Hipparcos and Tycho Catalogs*, (1997) SP-1200.

[2] B. Albayrak, *Ph. D. Thesis*, Ankara University, Graduate School of Nature and Applied Sciences, Department of Astronomy and Space Sciences, Ankara, Turkey, 1999.

[3] W. Buscombe, *ApJ*, (1951) 114, 73.

[4] C. Chadeau, *Ann d'Ap*, (1955) 18, 100.

[5] H. G. Groth, *Z. Astrophys.*, (1961) 51, 206.

[6] N. S. Taffara, *Mem. Soc. Astron. Ital.*, (1966) 37, 401.

[7] J. Zverko, *Bull. Astron. Inst. Czech.*, (1971) 22, 49.

[8] Z. A. Samedov, *Astron. Zh.*, (1993) 70, 82.

[9] Y. Takeda, M. Takada-Hidai and J. Kotake, *PASJ*, (1996) 48, 753.

[10] B. Albayrak, *A&A,* (2000) 364, 237.

[11] G. Hill, W. A. Fisher, *Publ. Dominion Astrophys. Obs.*, (1986) 16, No. 13.

[12] G. Hill, S. J. Adelman, *in Upper Main Sequence Stars with Anomolues Abundances*, (eds. C. R. Cowley et al.) (1986) Reidel, Dordrecht-Holland, p. 209.

[13] B. Albayrak, S. J. Adelman, A. F. Gulliver, D. A. Bohlender, C. Aydın and D. Koçer, (2000) in preparation.

[14] L. Achmad, H. J. G. L. M. Lamers, L. Pasquini, *A&A*, (1997) 320, 196.

[15] L. B. Lucy, *ApJ*, (1976) 206, 499.

[16] S. C. Wolff, *The A-Type Stars: Problems and Perspectives*, (1983) NASA SP-463 (NASA Washington D.C.).

[17] H. J. G. L. M. Lamers, L. Achmad, *A&A*, (1994) 291, 856.